

# Docking Method for Electric Vehicle Charging Terminal Using Monocular Camera

**Donghee Noh**

Korea Electronics Technology Institute

**Seonhyeong Kim**

Korea Electronics Technology Institute

**Seojeong Kim**

Korea Electronics Technology Institute

**Donghoon Kim**

Korea Electronics Technology Institute

**Kyoungho Choi**

Econexon

**Juhwan Choi**

Korea Electronics Technology Institute

**Keunho Park** (✉ [root@keti.re.kr](mailto:root@keti.re.kr))

Korea Electronics Technology Institute

---

## Research Article

**Keywords:** Machine vision, Artificial intelligence, electric vehicle charging, Articulated robot

**Posted Date:** August 8th, 2023

**DOI:** <https://doi.org/10.21203/rs.3.rs-3180077/v1>

**License:**  This work is licensed under a Creative Commons Attribution 4.0 International License.

[Read Full License](#)

---

# Abstract

With the growth of battery-based eco-friendly electric vehicle parts and materials technology, the diversity of smart EV-related industries is increasing. However, the lack of rapid charging stations, which hinders the growth of the eco-friendly electric vehicle market, is approaching as a realistic problem. Various companies such as Volkswagen, EVAR, KUKA, MOBI, CarLa, and TESLA are competing to develop and commercialize unmanned automated electric vehicle charging robots using robots to solve the shortage of charging stations and the inconvenience of charging electric vehicles for the physically weak such as children and the elderly. This paper conducted a study on docking and undocking the charging terminal of a battery cart to the charging terminal of an electric vehicle using hardware consisting of a monocular camera, an articulated robot, a gripper, and a server among unmanned automated electric vehicle charging systems. In order to evaluate the performance of the system, an experiment was conducted to evaluate the success rate of docking and undocking tasks, and the average success rate of 99% was derived as a result of the experiment.

## 1 Introduction

With the growth of battery-based eco-friendly electric vehicle parts and materials technology, the diversity of smart EV-related industries is increasing [1]. However, the lack of rapid charging stations, which hinders the growth of the eco-friendly electric vehicle market, is approaching as a realistic problem [2–3]. In Korea, a bill to ban sales of internal combustion engine vehicles by 2030 has been submitted to the National Assembly, and the growth of smart EV and electric vehicle parts related industries is expected due to the growth of battery-based eco-friendly electric vehicle parts and materials technology [4]. The growth of related industries will be accelerated through government policy support, technology and business support to improve the environment and create next-generation innovative growth engines.

The performance of core parts such as batteries and driving systems has been improved to increase the mileage on a single charge to more than 500 km through steady technology development to improve battery capacity and efficiency for electric drive platforms. In addition, the development of supercharger technology, such as high-voltage cables, connectors, and converters, is actively under way to improve motor and inverter technology, which determine driving performance, increase charging capacity, and reduce time [5–7]. Trends in electric vehicles, small electric trucks, agricultural transport carts, wheelchairs, commercially equipped vehicles, and construction machinery industries are also changing to forms using electric drives [8].

Volkswagen has set the concept for an electric vehicle automatic charging system, but it has not yet been commercialized [9]. In order to automatically charge electric vehicles, we are planning to develop mobile robots and mobile energy storage carts. The mobile energy storage cart has a capacity of 25 kWh and a 50 kW fast charger, and serves to charge the electric vehicle. The mobile robot plays the role of moving the energy storage cart to the location of the electric vehicle and connecting the mobile energy storage cart and the electric vehicle. EVAR, a start-up venture of Samsung Electronics' C-Lab., has developed an

automatic charging system for electric vehicles, but this has not yet been commercialized [10]. It is a product that combines an energy storage device and a mobile robot to autonomously charge an electric vehicle. In addition, companies such as 'KUKA', 'MOBI', 'CarLa', and 'TESLA' [9] are competing to develop and commercialize unmanned automated electric vehicle charging robots using robots.

This paper conducted a study on docking or undocking the charging terminal of a battery cart to the charging terminal of an electric vehicle using hardware consisting of a monocular camera, an articulated robot, a gripper, and a server among unmanned automated electric vehicle charging systems. A square-shaped landmark with a specific size is attached to the charging terminal so that the precise phase can be recognized even with a monocular camera using the PPE algorithm. Recognized information of the charging terminal analyzed by the server is transmitted to the articulated robot and the gripper through the TCP/IP communication protocol to perform docking and undocking operations.

## 2 Problem Background

### 2.1 Coordinate system

In order to recognize a target such as a charging terminal using a camera and transfer the geometrical information of the target to the hardware of another module such as an articulated robot to perform a task, an understanding of spatial information, that is, a coordinate system is required [11]. Coordinate systems commonly used in camera models can be divided into four types: world coordinate system, camera coordinate system, pixel coordinate system, and regular coordinate system.

The world coordinate system refers to a coordinate system that is used as a reference when expressing the position of an object in a 3-dimensional coordinate system, and can be expressed as in Eq. 1.

$$\mathbf{p}_w = (X, Y, Z)$$

1

This coordinate system can be arbitrarily set and used by the user according to the problem. In this study, the world coordinate system was set based on the gripper that grips the charging terminal.

The camera coordinate system can be expressed as Eq. 2 in a 3-dimensional coordinate system such as the world coordinate system.

$$\mathbf{p}_c = (X_c, Y_c, Z_c)$$

2

If the world coordinate system can be arbitrarily set by the user and can be modified, the camera coordinate system cannot be modified because it is based on the lens of the camera. With the focal point of the camera, which is the center of the lens, as the origin, the optical axis direction in front of the

camera is the  $z$ -axis, the downward direction of the camera is the  $y$ -axis, and the right-hand direction is the  $x$ -axis. By correlating the camera coordinate system and the world coordinate system, the two coordinate systems can be moved with extrinsic parameters expressed as rotation and translation transformations between the two coordinate systems.

The pixel coordinate system is a 2-dimensional coordinate system, also called an image coordinate system, and can be expressed as Eq. 3.

$$\mathbf{p}_{img} = (x, y)$$

3

As a coordinate system for an image viewed by the naked eye, the left-top corner of the image is the origin, the right direction is the  $x$ -axis increment direction, and the downward direction is the  $y$ -axis increment direction.

The normal coordinate system is a 2-dimensional coordinate system. All three coordinate systems mentioned above are intuitive coordinate systems, but the normal coordinate system is a virtual coordinate system introduced for convenience and can be expressed as in Eq. 4.

$$\mathbf{p}' = (u, v)$$

4

It is a coordinate system in which the influence of the camera intrinsic parameter matrix  $\mathbf{K}$  is removed from the pixel coordinate system, and it is a coordinate system that defines a virtual image plane whose distance from the camera focal point is 1.

$$\mathbf{K} = \begin{bmatrix} f_x & skew_x & c_x \\ 0 & f_y & c_y \\ 0 & 0 & 1 \end{bmatrix}$$

5

Where,  $f_x$  and  $f_y$  represent the effective focal length (in pixels) of each of  $x$  and  $y$  axes,  $c_x$  and  $c_y$  represent the principal point of the camera on each of  $x$  and  $y$  axes, and  $skew_x$  represents the tilt of the camera. The origin of the normal coordinate system is the midpoint of the normal image plane, which is also the point of intersection with the optical axis.

## 2.2 Lens distortion correction

If you use a wide-angle lens with a wide field of view (FOV) or an ultra-wide-angle lens such as a fisheye lens, you can see a wide range, but this causes a problem of relatively severe image distortion [12]. In addition to visual problems, this image distortion is particularly problematic when accurate numerical

calculation is required through image analysis. For example, if image coordinates are converted into world coordinates in order to know the actual position of an object detected in an image, a serious error will occur depending on the degree of image distortion. There are two major types of distortion caused by the physical characteristics of the lens and the assembly method of the camera: radial distortion and tangential distortion.

Radial distortion is caused by the refractive index of a convex lens and is a distortion in which the degree of distortion of an image is determined by the distance from the center. In general, the mathematical model of lens distortion is defined in a normal coordinate system in which the influence of camera parameters is removed. Since radial distortion does not occur at all in the center of the image sensor and occurs more toward the periphery, it can be expressed using a Taylor series. Equations representing radial distortion are as Eqs. 6 and 7.

$$u_{u\_r} = u_{d\_r} (1 + k_1 r^2 + k_2 r^4 + k_3 r^6)$$

6

$$v_{u\_r} = v_{d\_r} (1 + k_1 r^2 + k_2 r^4 + k_3 r^6)$$

7

Where,  $u_{d\_r}$  and  $v_{d\_r}$  denote original positions of distorted points,  $u_{u\_r}$  and  $v_{u\_r}$  denote new corrected positions,  $k_1$ ,  $k_2$  and  $k_3$  denote radial distortion coefficients, and  $r$  represents the distance from each point to the centroid.

Tangential distortion is distortion that occur when the camera lens (CCD) and the image sensor (CMOS) are not leveled or the lens itself is not centered during the camera manufacturing process, and the distortion distribution changes in an elliptical shape. This is also defined in the normal coordinate system. Equations representing the tangential distortion are Eqs. 8 and 9.

$$u_{u\_t} = u_{d\_t} (2p_1 v_{d\_t} + p_2 (r^2 + 2u_{d\_t}^2))$$

8

$$v_{u\_t} = v_{d\_t} (2p_2 u_{d\_t} + p_1 (r^2 + 2v_{d\_t}^2))$$

9

Where,  $u_{d\_t}$  and  $v_{d\_t}$  denote the original position of the distorted point,  $u_{u\_t}$  and  $v_{u\_t}$  denote the new corrected position,  $p_1$  and  $p_2$  denote the tangential distortion coefficients, and  $r$  are the respective It represents the distance from a point to the center.

As mentioned above, since the mathematical model of lens distortion is defined in the normal coordinate system, camera coordinates (Eq. 3) are converted into normal coordinates (Eq. 4) through multiplication

with the inverse matrix  $K^{-1}$  of camera intrinsic parameters (Eq. 5) to remove distortion. In addition, the distortion is corrected by applying Eq. 6–9, and then converted back to camera coordinates through multiplication with  $K$ , so that the image with the distortion removed can be visually expressed.

## 2.3 ArUco marker

The ArUco marker is a composite square marker consisting of a wide black border and an internal binary matrix that determines an identifier (id) [13]. Black borders facilitate fast detection in images, and binary coding allows identification and application of error detection and correction techniques. The size of the matrix inside the marker determines the amount of data the marker can represent. For example, a marker size of 4x4 can represent 16 bits and can represent numbers from 0 to 65,535. The markers can be found rotated according to the camera's shooting direction, but the detection process must clearly identify each corner, and this is done based on binary coding. A binary coded list according to marker shapes defined for each specific application is called a marker dictionary. Based on the information in the marker dictionary, markers used for detection can be created.

The process of detecting markers is divided into five steps: binarization, contour extraction, perspective transformation, grid segmentation, and information extraction. First, the input image is converted into a gray-scale image, and then the image is binarized by applying adaptive thresholding. The reason why the Otsu binarization method is not performed here is that the Otsu binarization performs unstable binarization according to the shade and outputs light-sensitive results. Second, when binarization is completed, marker candidates are filtered based on the information of the detected figures of the image. Information on figures can be obtained by extracting contours. In the case of a figure with 4 vertices and a convex polygon (only a rectangle satisfies the two conditions), it is left as a marker candidate. Thirdly, perspective transformation is performed using the four vertex information obtained in the contour extraction process. The reason for performing the perspective conversion is to remove the distortion of the marker according to the perspective. The marker candidate from which the distortion has been removed performs the fourth process of grid segmentation. After grid division of marker candidates based on the size of the marker, which is prior information, the ratio of white and black (there are only two colors because the image is binarized) is determined in the grid area, and if there is a lot of white, the area is 1 and black. If there are many, the area is replaced with 0. Finally, information is extracted by arranging the replaced information in a row. According to this information, the rotation information of the marker can be grasped, the position of the upper left corner of the marker can be grasped, and the identifier of the marker can be read.

## 2.4 Plain-based pose estimation

Plane-based pose estimation (PPE), which estimates the pose of a plane given a series of point correspondences, is a fundamental problem in computer vision and the basis for many important applications.

The core meaning of PPE means estimating a model that matches the information of the plane included in the image with the 3D coordinate information of the actual plane [14]. Applications of PPE include

estimating poses of textured planar surfaces seen in video, or using planar markers to perform AR. Another important application of PPE is to estimate camera eigenvalues by camera calibration, then perform PPE to obtain camera eigenvalues, and then perform eigenvalue refinement through a combination of intrinsic/extrinsic parameters. Methods for addressing PPE can be divided into two main categories. Methods for addressing PPE can be divided into two main categories. The first is a method to solve the PPE by decomposing the related plane-to-view homography, and this method is called a HD (Homography Decomposition) method. The second treats PPE as a special case of the general fixed pose estimation problem in point correspondence. When the camera is in perspective, this is known as a PnP problem, where  $n$  represents a corresponding number. HD works by exploiting the fact that the transforms induced by the perspective or affine projection of a plane are homographs. Once the estimated homography is decomposed by a matrix decomposition method such as singular value decomposition (SVD), very efficient pose estimation can be provided. The PnP method optimizes the pose using a cost function related to the correspondence transfer error. The PnP method optimizes the pose using a method that minimizes a correspondence transfer error. Research on PnP has focused on solving problems with  $n = 3$  and  $n = 4$  special cases and random  $n$ . Both methods of decomposing homography or minimizing correspondence propagation errors can define a cost function Eq. 10 that minimizes the error of comparing the locations of measured points with those of corresponding predicted locations.

$$s \begin{bmatrix} u \\ v \\ 1 \end{bmatrix} = \mathbf{K} [\mathbf{I}_3 \quad 0] \begin{bmatrix} \mathbf{R} & \mathbf{t} \\ \mathbf{0}^\top & 1 \end{bmatrix} \begin{bmatrix} X \\ Y \\ Z \\ 1 \end{bmatrix} = \mathbf{K}\lambda\mathbf{H} \begin{bmatrix} X \\ Y \\ Z \\ 1 \end{bmatrix}$$

9

Where,  $\mathbf{I}_k$  denotes a  $k \times k$  identity matrix,  $\mathbf{R}$  denotes a rotation matrix  $[\mathbf{r}_1 \quad \mathbf{r}_2 \quad \mathbf{r}_3]$ , and  $\mathbf{t}$  denotes a translation vector. Since noise is added when  $\mathbf{H}$  is observed with a camera, the cost function applying  $\widehat{\mathbf{H}}$  with noise  $\epsilon_H$  added is as follows.

$$\min_{\mathbf{r}_1, \mathbf{r}_2, \mathbf{r}_3, \mathbf{t}} \|\lambda \widehat{\mathbf{H}} - [\mathbf{r}_1 \quad \mathbf{r}_2 \quad \mathbf{r}_3 \quad \mathbf{t}] \|_2^2 \quad \text{s.t. } [\mathbf{r}_1 \quad \mathbf{r}_2 \quad \mathbf{r}_3]^\top [\mathbf{r}_1 \quad \mathbf{r}_2 \quad \mathbf{r}_3] = \mathbf{I}_3$$

10

### 3 Docking Method for Electronic Vehicle Charging Terminal

The hardware components including the articulated robot, charging terminal gripper, monocular camera, charging terminal, and charging terminal holder used in this study are shown in Fig. 1. Figure 1 (a) is an electric vehicle charging robot towing a battery cart. It consists of an articulated robot, a charging terminal gripper, and a monocular camera set that performs docking and undocking of charging terminals in front of the body of the electric vehicle charging robot. A monocular camera recognizes the landmark attached to the charging terminal, and the docking and undocking of the charging terminal is

performed by the motion of the articulated robot and the charging terminal gripper. The battery cart towed by the electric vehicle charging robot consists of a holder (Fig. 1 (d)) that fixes the charging terminals on the battery cart when the electric vehicle is not being charged, and a charging terminal on the electric car side (Fig. 1 (c)) connected to the battery with wires and a charging terminal on the battery cart side that performs charging. Figure 1 (b) is the charging terminal of the electric vehicle side that the user of the electric vehicle charging system attaches to his or her charging port when requesting charging of the electric vehicle.

---

#### ALGORITHM 1: Procedure of Charging Terminal Docking

---

```
check articulated robot and gripper operation
check camera calibration resources and operation
receive image from camera
remove lens distortion in the image using camera calibration resources
while there is no landmark in the image, do
    moves an articulated robot in an arbitrary direction and angle
    receive image from camera
    remove lens distortion in the image using camera calibration resources
end
calculate landmark translation vector t and , rotation matrix R using PPE
calculate the values of landmark translation variables [ $t_x, t_y, t_z$ ], inclination variables [ $r_{pan}, r_{tilt}, r_{roll}$ ]
dock the charging terminal by operating the articulated robot using variables  $t_x, t_y, t_z, r_{pan}, r_{tilt}, r_{roll}$ 
start to electric vehicle charge
```

---

Charging terminal docking for unmanned and automated electric vehicle charging is performed in the same way as in Algorithm 1. First, the operation of hardware such as an articulated robot, gripper, and monocular camera necessary for docking the charging terminal, and camera calibration resources containing camera intrinsic and extrinsic parameters and distortion coefficient information for lens distortion correction are checked. If there is no problem with the hardware and camera calibration resources, it starts receiving images from the monocular camera. The analysis performance is improved by removing tangential distortion and radial distortion from the received image using camera internal parameters. If a landmark is detected in the distortion-free image and the landmark is not found, a series of processes ‘move the articulated robot in arbitrary direction and angle’, ‘receive video’, ‘remove image distortion’, and ‘looking for landmarks’ are repeated until the landmark is found. Here, the landmarks used ArUco markers. If a marker is detected during the iterative process, the iteration is stopped and the translation vector **t** and rotation matrix **R** corresponding to the marker’s perspective information are calculated using the PPE method based on the vertex information of the marker. Finally, docking and undocking can be performed by transmitting  $t_x, t_y, t_z$  corresponding to each element of **t** and  $r_{pan}, r_{tilt}, r_{roll}$  calculated using Euler-Rodrigues formula based on **R** to the articulated robot.

## 4 Experimental Result

## 4.1 Hardware configuration

The articulated robot used in the experiment is Doosan Robotics' A0912 model, which has a payload of 9kg, a working radius of 1200mm, and a repeat accuracy of  $\pm 0.05\text{mm}$ . The charging terminal gripper is OnRobot's RG2 v2, which has a payload force fit of 2kg, a payload form fit of 5kg, and a total stroke of 110mm. The monocular camera is the SQ13, which has a 155° FoV, 1920×1080 resolution, and a frame rate of 30 fps. The server is a model called ASUS MiniPC PB60G and has a CPU i5-9400T, GPU GTX1650, 8G RAM, and 256GB of storage. The rest of the hardware, such as the charging terminal and the charging terminal stand, was produced by ourselves. The communication structure is shown in Fig. 2. Since a monocular camera is connected to the server via USB, the server analyzes the video received from the monocular camera, and the server and the articulated robot are connected via a LAN port, so the analysis result is transmitted through TCP/IP communication. The articulated robot and the charging terminal gripper are also connected through a LAN port and perform TCP/IP communication.

## 4.2 Charging terminal recognition rate and recognition speed

In order to understand the performance of the charging terminal docking system, an experiment was conducted to evaluate the charging terminal recognition rate and charging terminal recognition speed. The charging terminal recognition rate was evaluated by calculating the rate of accurately recognizing the charging terminal within the detection range (1m), and the calculation method is as follows.

$$\text{recognitionrate} = \frac{\text{Equation Number of successes}}{\text{Equation Number of experiments}}$$

11

Similarly, the charging terminal recognition speed is evaluated by the detection time when the charging terminal within the detection range (1m) is successfully detected, and the calculation equation is as follows.

$$\text{recognition speed} = \text{recognition success time} - \text{recognition start time}$$

12

The visualization program developed for the experiment is shown in Fig. 3. When a landmark is recognized, the recognition result is displayed in the upper left corner of the visualization program, and the recognition speed is displayed in the upper right corner. The simulation results of electric vehicle side charging terminal, battery cart side charging terminal, and battery cart side charging terminal holder are displayed, respectively, as shown in (a), (b), and (c) of Fig. 3 centering on the landmark. In the case of the charging terminal holder, it also contains a landmark to be recognized, so it was included after experimentation. For each of the three charging terminals, 50 experiments were conducted, and the results of the experiments are shown in Tables 1 and 2.

Charging terminal recognition success rate test results showed a recognition success rate of 96% for case of electric vehicle side charging terminal, 100% recognition success rate for case of battery cart side charging terminal, and 98% recognition success rate for case of battery cart side charging terminal holder, indicating an overall average of 98% recognition success rate.

As a result of the charging terminal recognition speed test, the recognition speed was 0.0117 seconds for electric vehicle side charging terminal, 0.0083 seconds for battery cart side charging terminal, and 0.0097 seconds for battery cart side charging terminal holder, indicating an average recognition speed of 0.0099 seconds.

**Table 1**  
**Result of charging terminal recognition success rate test**

<b>Kind</b>	<b>Number of experiments</b>	<b>Number of successes</b>	<b>Charging terminal recognition rate (%)</b>
Electric vehicle side charging terminal	50	48	96.00
Battery cart side charging terminal	50	50	100.00
Battery cart side charging terminal holder	50	49	98.00
Total	150	147	98.00

**Table 2**  
**Result of charging terminal recognition speed test**

<b>Kind</b>	<b>Number of experiments</b>	<b>Charging terminal recognition speed average (sec)</b>
Electric vehicle charging terminal	50	0.0117
Battery cart side charging terminal	50	0.0083
Battery cart side charging terminal holder	50	0.0097
Total	150	0.0099

In order to evaluate the completeness of the charging terminal docking system, the charging terminal docking and undocking success rates were evaluated. The process of docking and undocking is shown in Fig. 4. First, as in step 1, the articulated robot moves near the battery cart side charging terminal and searches for the battery cart side charging terminal. When the search is completed as in step 2, grip the battery cart side charging terminal using the gripper. When the grip is completed, the battery cart side charging terminal moves to the electric vehicle side charging terminal or the battery cart side charging terminal holder as in step 3. After moving, the battery cart side charging terminal searches for the electric

vehicle side charging terminal or battery cart side charging terminal holder as in step 4. When the search is completed as in step 5, the articulated robot combines the battery cart side charging terminal with the electric vehicle side charging terminal or the battery cart side charging terminal holder, and the process is completed as in step 6.

The experiment was conducted by calculating the success rate by performing docking and undocking 50 times each, and the experimental results are shown in Table 3. As a result of the docking test of the charging terminal, the success rate was 98%, and the case of undocking was 100%, showing an overall average success rate of 99%.

Table 3  
Result of charging terminal docking and undocking success rate test

Kind	Number of experiments	Number of successes	Success rate (%)
Charging terminal docking	50	49	98.00
Charging terminal undocking	50	50	100.00
Total	100	99	99.0

## 5 Conclusion

This paper conducted a study on docking or undocking the charging terminal of a mobile battery to the charging terminal of an electric vehicle using hardware consisting of a monocular camera, an articulated robot, a gripper, and a server among unmanned automated electric vehicle charging systems. A square-shaped landmark with a specific size is attached to the charging terminal so that the precise phase can be recognized even with a monocular camera using the PPE algorithm. Recognized information of the charging terminal analyzed by the server is transmitted to the articulated robot and the gripper through the TCP/IP communication protocol to perform docking and undocking operations. In order to evaluate the performance of the system, an experiment was conducted to calculate the charging terminal recognition rate and recognition speed. As a result of the experiment, the average charging terminal recognition rate was 98% and the average charging terminal recognition speed was 0.0099 seconds. In addition, an experiment was conducted to evaluate the docking and undocking success rate to evaluate the performance of docking and undocking tasks, and the average success rate of 99% was derived as a result of the experiment.

## Declarations

### ACKNOWLEDGMENTS

This work was supported by Industrial Technology Innovation Project, funded by Ministry of Trade, Industry and Energy (No.20023014)

### CONFLICT OF INTEREST

This manuscript has not been published or presented elsewhere in part or in entirety and is not under consideration by another journal. We have read and understood your journal's policies, and we believe that neither the manuscript nor the study violates any of these. There are no conflicts of interest to declare. All authors have approved the manuscript and agree with its submission to International Journal of Intelligent Robotics and Applications.

## DATA AVAILABILITY STATEMENT

The datasets used and/or analysed during the current study available from the corresponding author on reasonable request.

## References

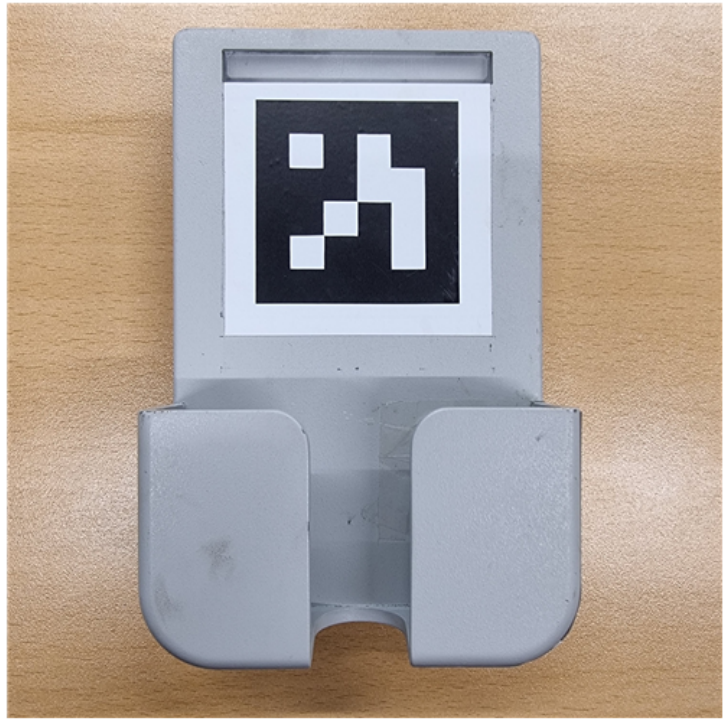
1. D. B. Richardson, "Electric vehicles and the electric grid: A review of modeling approaches, Impacts, and renewable energy integration," Renewable and Sustainable Energy Reviews, vol. 19, pp. 247-254, 2013.
2. O. Sin, "Electric vehicle charging infrastructure technology trends," The Korean Institute of Power Electronics, vol. 27, pp. 28-35, 2022.
3. S. Kwon, "Global electric vehicle trends and our strategy," Auto Journal, vol. 43, no. 9, pp. 35-38, 2021.
4. N. Huh, "In the era of climate crisis, eco-friendly vehicles open the future of the automobile industry," Korea Research Institute for Human Settlements, vol. 473, pp. 2-4, 2021.
5. B.U. Kim, "Electric Vehicle Technology Trend," The Korean Institute of Electrical Engineers, vol. 62, pp. 15-20, 2013.
6. J.H. Choi, "Recent Technology Trend of Traction Inverter for Electric Vehicles," Auto Journal, vol. 39, pp. 25-28, May 2017.
7. W. Lee, E. Schubert, Y. Li, S. Li, D. Bobba and B. Sarlioglu, "Overview of Electric Turbocharger and Supercharger for Downsized Internal Combustion Engines," IEEE Transactions on Transportation Electrification, vol. 3, pp. 36-47, March 2017.
8. Y. Son and K. Heo, "Technology Development Trend of Domestic and Foreign Electric Vehicle and Technology Development Strategy of Domestic Electric Vehicle Core Parts," The Transactions of the Korean Institute of Power Electronics, vol.22, pp. 373-381, October 2017.
9. A. K. Güngör and I. Kiyak, "Automatic Charging of Electric Driverless Vehicles with Robotic Arm," 2021 Innovations in Intelligent Systems and Applications Conference (ASYU), Elazig, Turkey, 2021, pp. 1-6.
10. Bjorn Nyland, EVAR - autonomous charging robot by Samsung [Video file], September 2018, [online] Available: <https://www.youtube.com/watch?v=50n-fx-mjw>.
11. Y. Ho, "Acquisition and processing technology of multi-view 3D image," Journal of the Electronic Engineering Society, vol. 40, no. 3, pp. 18-27, 2013.
12. J. Park, S. -C. Byun and B. -U. Lee, "Lens distortion correction using ideal image coordinates," in IEEE Transactions on Consumer Electronics, vol. 55, no. 3, pp. 987-991, Aug. 2009.

13. H. C. Kam, Y. K. Yu and K. H. Wong, "An Improvement on ArUco Marker for Pose Tracking Using Kalman Filter," 2018 19th IEEE/ACIS International Conference on Software Engineering, Artificial Intelligence, Networking and Parallel/Distributed Computing (SNPD), Busan, Korea (South), 2018, pp. 65-69.
14. Collins, T., Bartoli, A. "Infinitesimal Plane-Based Pose Estimation," *Int J Comput Vis*, vol. 109, pp. 252–286, 2014.
15. (Aug. 2015). Charger Prototype Finding Its Way to Model S. [Online]. Available: <https://www.youtube.com/watch?v=uMM0IRfX6YI>

## Figures



(a)



(b)



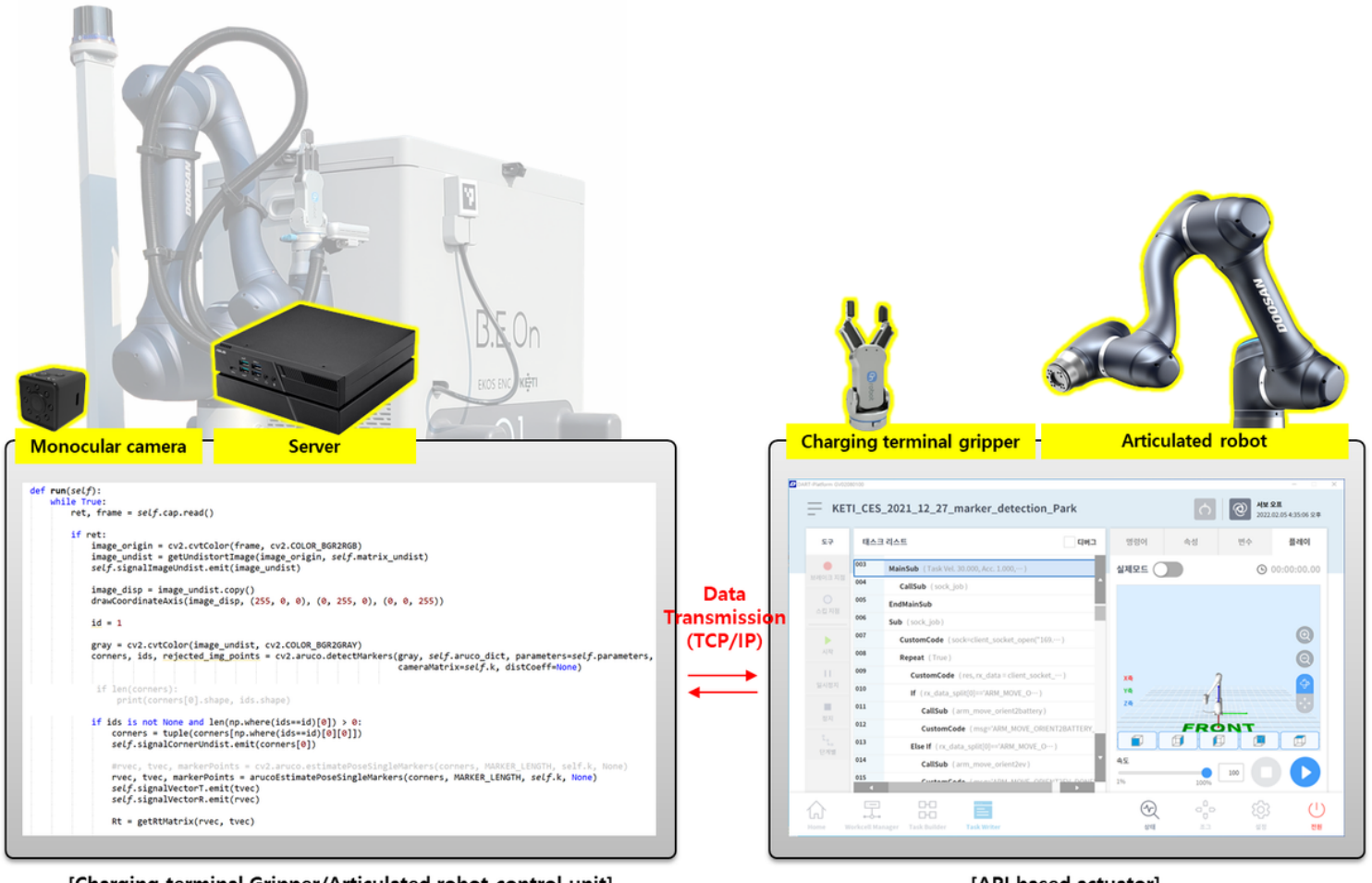
(c)



(d)

**Figure 1**

Hardware components for electric vehicle charging. (a) An electric vehicle charging robot and battery cart with elements such as an articulated robot, a charging port gripper, a monocular camera, and a charging terminal. (b) Electric vehicle side charging terminal. (c) Battery cart side charging terminal. (d) Battery cart side charging terminal holder.

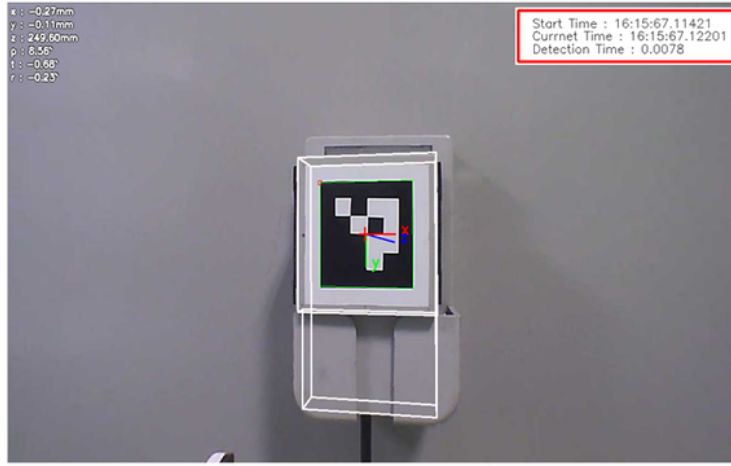


[Charging terminal Gripper/Articulated robot control unit]

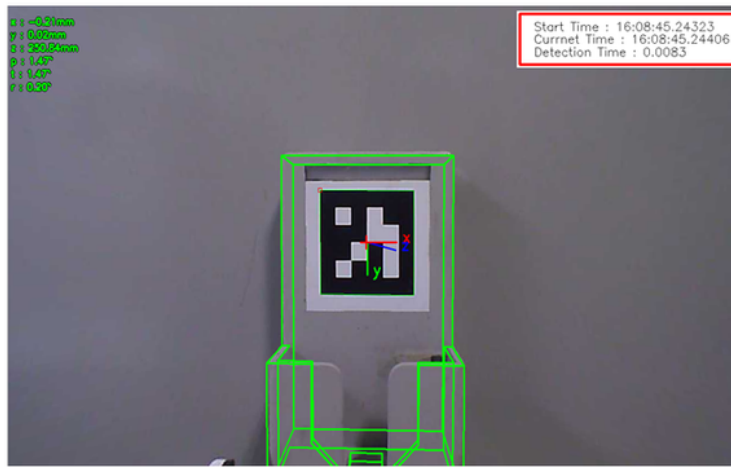
[API based actuator]

Figure 2

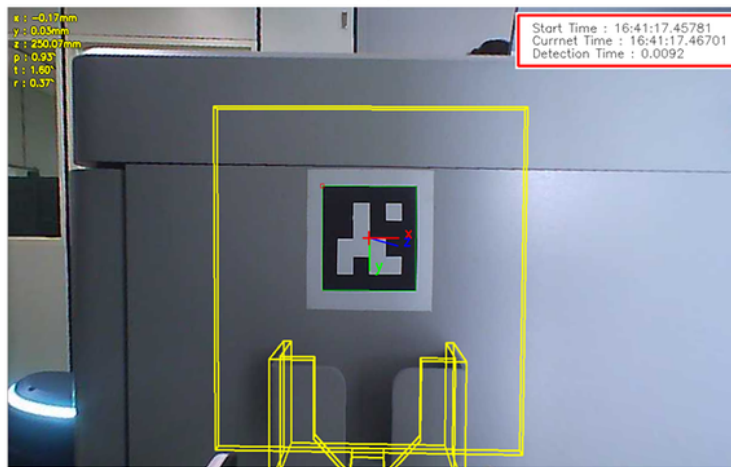
Communication structure of charging terminal docking system.



(a)



(b)



(c)

Figure 3

Visualization program and recognition results for charging terminal recognition rate and charging terminal recognition speed evaluation. (a) Electric vehicle side charging terminal recognition result. (b) Battery cart side charging terminal recognition result. (c) Battery cart side charging terminal holder recognition result.

Stage	Action	Charging terminal docking	Charging terminal undocking
1	Mounted charging terminal detection		
2	Mounted charging terminal grip		
3	Moving the charging terminal after completing the grip		
4	Charging terminal holder detection		
5	Mount the charging terminal		
6	Charging terminal mount complete		

**Figure 4**

Charging terminal docking and undocking performance test. The 1<sup>st</sup> column indicates the steps taken. The 2<sup>nd</sup> column shows a description of each step. The 3<sup>rd</sup> column shows examples of each step for charging terminal docking. The 4<sup>th</sup> column shows examples of each step for charging terminal undocking.